Multimodal Molecular Imaging of Integrin $\alpha_v\beta_3$ for In Vivo Detection of Pancreatic Cancer

Marija Trajkovic-Arsic[1], Pouyan Mohajerani[2], Athanasios Sarantopoulos[2], Evdokia Kalideris[1], Katja Steiger[3], Irene Esposito[3], Xiaopeng Ma[2], George Themelis[2], Neal Burton[2], Christoph W. Michalski[4], Jörg Kleeff[4], Stefan Stangl[5], Ambros J. Beer[6], Karolin Pohle[6,7], Hans-Jürgen Wester[7], Roland M. Schmid[1], Rickmer Braren[8], Vasilis Ntziachristos[2], and Jens T. Siveke[1]

[1]II. Medizinische Klinik, Klinikum rechts der Isar, Technische Universität München, Munich, Germany; [2]Technische Universität & Helmholtz Zentrum München, Neuherberg, Germany; [3]Institut für Pathologie, Klinikum rechts der Isar, Technische Universität München, Munich, Germany; [4]Chirurgische Klinik, Klinikum rechts der Isar, Technische Universität München, Munich, Germany; [5]Experimentelle Radioonkologie und Strahlentherapie, Klinikum rechts der Isar, Technische Universität München, Munich, Germany; [6]Nuklearmedizinische Klinik, Klinikum rechts der Isar, Technische Universität München, Munich, Germany; [7]Pharmazeutische Radiochemie, Technische Universität München, Munich, Germany; and [8]Institut für Radiologie, Klinikum rechts der Isar, Technische Universität München, Munich, Germany

Pancreatic ductal adenocarcinoma (PDAC) is a lethal disease. Late detection of then nonresectable or metastasized tumors emphasizes the need for novel imaging approaches. Here, we report on so far nonexploited potentials of $\alpha_v\beta_3$ integrin–targeted molecular imaging technologies for detection of PDAC using genetically engineered mouse models. **Methods:** Immunohistochemistry and Western blot were used for characterization of $\alpha_v\beta_3$ expression in murine and human PDAC. We applied IntegriSense 680 fluorescence molecular tomography, intraoperative fluorescence imaging, and ^{68}Ga-NODAGA-RGD PET for $\alpha_v\beta_3$ integrin molecular in vivo imaging of spontaneous PDAC occurring in $Ptf1a^{+/Cre};Kras^{+/LSL-G12D};p53^{LoxP/LoxP}$ mice. (NODAGA is 1,4,7-triazacyclononane-1,4-bis[acetic acid]-7-[2-glutaric acid] and RGD is arginine-glycine-aspartic acid.) **Results:** $\alpha_v\beta_3$ integrin is expressed in tumor cells of human and murine PDAC. IntegriSense fluorescence molecular tomography and ^{68}Ga-NODAGA-RGD PET enabled faithful visualization of PDAC. Furthermore, intraoperative optical imaging with IntegriSense 680 allowed good delineation of tumor borders. **Conclusion:** Imaging approaches targeting $\alpha_v\beta_3$ integrin expand the potential of molecular imaging for identification of $\alpha_v\beta_3$-positive PDAC with potential implications in early detection, fluorescence-guided surgery, and therapy monitoring.

Key Words: integrin $\alpha_v\beta_3$; positron emission tomography; fluorescence molecular tomography; pancreatic cancer; genetically engineered mice

The devastating status of pancreatic ductal adenocarcinoma (PDAC) as the fourth most lethal human malignancy results from the late detection of often metastasized disease and resistance to chemotherapies (*1*). Thus, new imaging methods for detection, im-proved surgical resection, and clinically relevant therapy response monitoring are key aims to increase the survival in PDAC patients.

Clinically, PDAC diagnosis and determination of resectability are typically performed by imaging modalities such as MR imaging and CT, which provide information regarding tumor size, location, and morphology (*2*). Molecular imaging approaches that provide clinically meaningful additional information, such as subtypes or tumor biology, are not well established. Molecular imaging using ^{18}F-FDG and 3′-deoxy-3′-^{18}F-fluorothymidine PET has been recently characterized in humans, demonstrating high sensitivity for PDAC detection but low specificity with high rates of false-positive findings of inflammatory lesions or pseudomasses (*3,4*).

Among molecular imaging approaches, fluorescence-based optical methods are especially appealing because of their low-cost, high sensitivity and spatial resolution and absence of ionizing radiation (*5*). As such, fluorescence-guided surgery is increasingly used in operation rooms in which it allows precise visualization of targeted tissue and its margins during surgery (*6,7*).

Genetically engineered mouse models (GEMM) that faithfully recapitulate molecular and morphologic features of human PDAC have already been used successfully for translational diagnostic and therapeutic approaches including molecular imaging. Recent studies in GEMM reported on identification of cathepsins and Claudin 4 as promising molecular targets for in vivo detection of PDAC using fluorescence-based imaging technologies. These studies suggested that molecular imaging of suitable targets may allow identification of PDAC and precursor lesions and may thus be suitable for early detection methods (*8–11*). However, the tissue volume in humans limits some of the approaches reported because of signal attenuation.

In this paper, we identify $\alpha_v\beta_3$ integrin as a candidate target for visualization of PDAC. Integrin $\alpha_v\beta_3$ belongs to the integrin family of cell surface receptors expressed on activated endothelial cells of new sprouting vessels in the tumor but also on tumor cells in various cancers including PDAC (*12,13*). $\alpha_v\beta_3$ integrin has been implicated as a key player in tumor angiogenesis and metastasis and was shown to be especially relevant for the metastatic spread of PDAC to lymph nodes (*14,15*). Molecular imaging of $\alpha_v\beta_3$ integrin by RGD (H-Arg-Gly-Asp-NH$_2$; arginine-glycine-aspartic acid)–labeled PET tracers has been introduced into clinical prac-

tice and is used for visualization of angiogenesis in many cancers (*13,16,17*). However, its potential for PDAC imaging has not been addressed before.

Here, we report on the molecular imaging of $\alpha_v\beta_3$ integrin as a feasible and reliable approach for detection of PDAC and its high value for PDAC translational research. We report on robust $\alpha_v\beta_3$ expression in endogenous murine PDAC and in a subpopulation of human PDAC and demonstrate that detection of murine PDAC is achievable in vivo using $\alpha_v\beta_3$ integrin–targeted optical and PET imaging approaches.

MATERIALS AND METHODS

Animals

Animal strains and used mouse models have been previously described (*18–20*). Genetically engineered mice with pancreas-specific activation of oncogenic Kras^{G12D} and additional pancreas-specific deletion of p53 for development of invasive PDAC (*Ptf1a$^{+/Cre}$;Kras$^{+/LSL-G12D}$; p53$^{LoxP/LoxP}$*; referred to as *CKP* hereafter) were used. Animals were 5–7 wk old. All experiments were performed according to the guidelines of the local Animal Use and Care Committees.

Target Validation

Immunohistochemistry, immunofluorescence, and Western blot were performed on murine and human tissue samples according to standard protocols. A description of procedures and antibodies is given in the supplemental material (supplemental materials are available at http://jnm.snmjournals.org).

PET and Biodistribution Studies

One day before the PET scans, PDAC presence was confirmed via T2-weighted (T2w) MR imaging. Tumor-bearing *CKP* animals were injected with ^{68}Ga-labeled NODAGA (1,4,7-triazacyclononane-1, 4-bis[acetic acid]-7-[2-glutaric acid])-conjugated RGD peptide and scanned on a small-animal PET/CT scanner. Details on ^{68}Ga labeling of NODAGA-RGD are provided in the supplemental material. The small-animal PET and biodistribution studies were performed by tail-vein injection of 7–12 MBq of ^{68}Ga-NODAGA-RGD under isoflurane anesthesia. Static small-animal PET/CT scans were obtained using a combined PET/CT scanner (Inveon; Siemens). The scan was started 75 min after tracer injection (scan duration, 15 min). Image data were corrected for normalization, dead time, and decay. Images were reconstructed using a 2- and 3-dimensional ordered-subsets expectation maximum algorithm without scatter and attenuation correction. For anatomic information, axial PET images were fused to axial T2w MR images of corresponding animals, as the nonenhanced CT image from the PET/CT scanner was insufficient to distinguish tumor from surrounding soft-tissue structures because of low soft-tissue contrast. Images were analyzed using the Inveon Research Workplace (Siemens). For biodistribution experiments, animals were injected with ^{68}Ga-NODAGA-RGD and euthanatized, and blood and all internal organs were collected and wet-weighed 75 min after injection. The radioactivity was measured using a γ counter (Wallac Wizard, PerkinElmer). The results are presented as percentage injected dose per gram of tissue.

Optical Imaging Procedures

IntegriSense 680 (PerkinElmer), a commercially available small nonpeptide molecule labeled with near-infrared fluorochrome that specifically binds to $\alpha_v\beta_3$ integrin, was dissolved in phosphate-buffered saline, administered via tail vein bolus injection (2 nmol), and allowed to circulate for 24 h before all optical imaging experiments.

Fluorescence Molecular Tomography (FMT)

Mice were imaged in vivo using the FMT–CT (FMT-XCT) hybrid modality at Helmholtz Zentrum München (*21,22*). FMT-XCT operates in 360° full-ration geometry, where the mouse is illuminated by a scan-ning 670-nm laser at equispaced 24 gantry locations. Fluorescence and intrinsic images are obtained for every source position using a cooled charge-coupled device in transillumination mode. Optical and x-ray modules are located on perpendicular axes, which are both perpendicular to the animal axial direction. The system was mathematically modeled using a finite element method for modeling light propagation in tissue assuming homogeneous optical absorption and scattering coefficients of 0.2 and 15 cm^{-1} for the mouse tissue. The inverse problem was regularized using Tikhonov regularization and solved using the least-squares algorithm method. The FMT and CT acquisitions lasted 34 and 23 min, respectively, during which the mouse was kept under isoflurane-induced anesthesia.

Intraoperative Optical Imaging

At 24 h after injection of IntegriSense 680, a surgical incision exposed the abdominal cavity to the intraoperative imaging setup described previously (*23*), which captured color, intrinsic, and fluorescence images of the exposed pancreas and its surroundings, simulating an intraoperative imaging situation.

Ex Vivo Fluorescence Cryoslicing

For whole-mount cryoslicing, animals used for FMT-XCT and intraoperative imaging experiments were sacrificed and whole-mount-frozen after the experiment, cryosliced, and imaged with a cryoslicer modality (*24*). Axial cut color and fluorescence images were captured every 250 μm and then used to volumetrically visualize pancreas or tumor and surrounding tissues and to compare the fluorescence images with the corresponding T2w MR imaging axial images under the same geometry.

Competitive Studies

To eliminate the possibility of nonspecific deposition of ^{68}Ga-NODAGA-RGD in PDAC, around 400 μg of cilengitide, a selective $\alpha_v\beta_3$ inhibitor (*25*), were intravenously injected into animals 10–15 min before injections of ^{68}Ga-NODAGA-RGD, and biodistribution was performed as described.

For the competitive study, IntegriSense 680 (2 nmol) was intravenously injected into *CKP* animals with PDAC and allowed to circulate and occupy $\alpha_v\beta_3$ integrin sites for 24 h. Subsequently, ^{68}Ga-NODAGA-RGD was injected into the same animals and biodistribution performed as described.

RESULTS

$\alpha_v\beta_3$ Expression in Human PDAC

To investigate $\alpha_v\beta_3$ integrin expression in human PDAC, we performed immunohistochemistry for the integrin β3 subunit on 77 human PDAC specimens. Immunohistochemistry for β3 integrin identified 24 tumors as β3-positive (β$^+$) (31%) with staining within neoplastic, cancer cells. β3 staining was of cytoplasmic or membranous localization, and expression levels in tumor cells varied from low to high (Fig. 1A). Correlation between tumor grading and β3$^+$ positivity was not observed (data not shown).

$\alpha_v\beta_3$ Expression in Murine PDAC

We next analyzed expression of αv and β3 integrin subunits in the pancreas of wild-type mice and PDAC of *CKP* mice. As demonstrated by immunohistochemistry, in wild-type pancreas β3 expression was limited to occasional blood vessels whereas no staining was observed in the acinar or ductal compartments (Fig. 1B). In PDAC of *CKP* mice, a dramatic increase in staining signal was observed. β3$^+$ cells were numerous and scattered throughout the tumor, with expression in invasive ductal cancer cells and the surrounding stroma (Fig. 1B). Staining for cytokeratin 19 (CK19), an epithelial marker of cancer cells, and β3 on consecutive paraffin sections
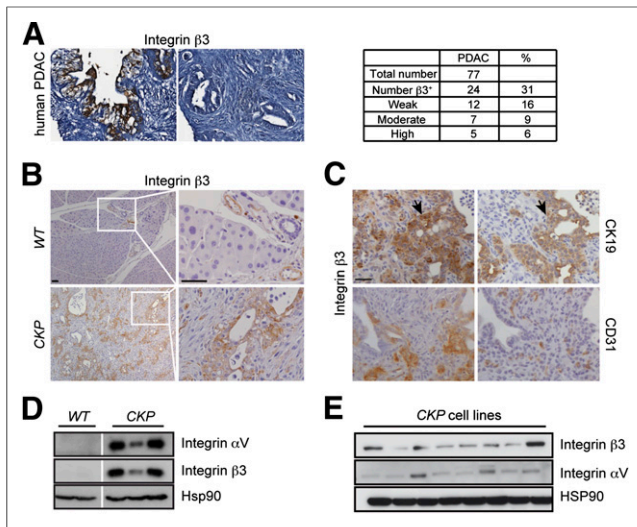
FIGURE 1. Expression analysis of $\alpha_v\beta_3$ integrin. (A) Human PDAC with membranous/cytoplasmatic and absent expression of integrin β3. Scale bar: 50 μm. Table summarizes β3 expression results for 77 human PDAC samples. (B) Immunohistochemistry for β3 integrin demonstrating no expression in wild-type pancreatic tissue and high expression in PDAC in *CKP* mice. Scale bars: 50 μm. (C) Immunohistochemistry for CK19, CD31, and integrin β3 on consecutive paraffin sections of murine PDAC demonstrating partial colocalization of CK19 and β3 integrin and different expression patterns of CD31 and β3 integrin. Scale bars: 50 μm. (D) Western blot analysis demonstrating higher αv and β3 expression in PDAC from *CKP* animals than healthy tissue from wild-type mice. Hsp90 served as loading control. (E) αv and β3 expression in primary *CKP* murine cancer cell lines demonstrated by Western blot analysis. Hsp90 served as loading control. WT = wild-type.

(Fig. 1C) supported β3 expression in cancer cells because a similar expression pattern of β3 and CK19 was observed. Immunohistochemistry staining on consecutive paraffin sections for β3 and CD31, a blood vessel marker, demonstrated that most β3$^+$ cells did not belong to tumor vessels (Fig. 1C). Western blot analysis demonstrated an increased expression of both αv and β3 protein subunits in PDAC, compared with wild-type pancreas (Fig. 1D). Furthermore, Western blot analysis of primary cancer cell lines isolated from tumors of *CKP* mice revealed that both αv and β3 were expressed in all 8 tumor cell lines isolated from different animals, albeit at different levels (Fig. 1E).

$\alpha_v\beta_3$-Targeted FMT and PET

Motivated by high $\alpha_v\beta_3$ expression, we implemented 2 different $\alpha_v\beta_3$-targeted molecular imaging methods and compared their efficiencies and benefits for PDAC detection: PET with ^{68}Ga-NODAGA-RGD probe as an approach in clinical use and FMT-XCT with IntegriSense 680 probe as a novel strategy for imaging PDAC.

Positive PET signals were clearly detectable in PDAC (Fig. 2A), although delineation of cancer borders on PET images was not good because of the intrinsically low spatial resolution. To validate PET results, a biodistribution assay was performed. High accumulation of ^{68}Ga-NODAGA-RGD in PDAC was detected (Fig. 2B). Competitive studies with $\alpha_v\beta_3$ inhibitor cilengitide showed that the amount of radioactivity accumulated in PDAC after cilengitide injections was dramatically lower than radioactivity measured in PDACs without cilengitide injections (Fig. 2C).

In animals bearing PDAC, we showcased a previously undocumented capability of FMT-XCT in 3-dimensionally resolving strong

fluorescence signals localized specifically in pancreatic tumor (Fig. 3; Supplemental Video 1). Strong fluorescence signals were detected in PDAC, demonstrating the superiority of FMT-XCT to PET in this case.

Intraoperative Imaging

Because of high PDAC fluorescence in FMT-XCT experiments, we hypothesized that intraoperative detection of PDAC via IntegriSense fluorescence would be possible. As previously published in wild-type animals (*24*), no fluorescence was detectable from the surface of the healthy pancreas, suggesting no specific accumulation of IntegriSense in normal pancreatic tissue (Fig. 4A). In *CKP* animals, PDACs were remarkably well visualized, showing strong and specific fluorescence signals from tissue surface (Fig. 4A). Fluorescence contrast to the adjacent tissues and thus demarcation of tumor borders was conspicuous. High near-infrared fluorescence signals were detected only at the tumor surface, indicating specific IntegriSense accumulation in the tumor. Examination of other exposed organs showed some fluorescence signals arising primarily from the gut, stomach, fat pads, urinary bladder, and ovaries in females. The liver showed no increased signals.

To confirm that IntegriSense 680 indeed binds to $\alpha_v\beta_3$ integrin in PDAC, we performed a competitive binding experiment with ^{68}Ga-NODAGA-RGD (Fig. 4B). The preinjection of IntegriSense dramatically decreased the amount of ^{68}Ga-NODAGA-RGD that accumulated in PDAC.
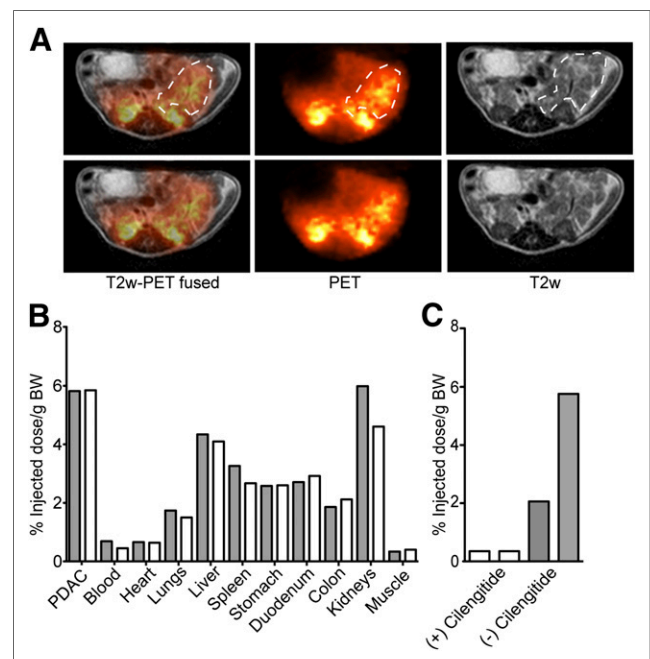

FIGURE 2. ^{68}Ga-NODAGA-RGD PET detects PDAC in vivo. (A) Fused and single axial T2w MR and ^{68}Ga-NODAGA-RGD PET images of PDAC. Positive PET signal in orange is present in tumor and kidneys. In images, tumor is delineated with white dotted line (upper) and without delineation for readers' comfort (lower). Kidneys show positive PET signals due to clearance of ^{68}Ga-NODAGA-RGD through kidneys. (B) Biodistribution of ^{68}Ga-NODAGA-RGD demonstrating accumulation of radioactivity in PDAC in *CKP* animals. Results from 2 animals are presented (gray bar, animal 1; white bar, animal 2). (C) Preinjection of cilengitide decreases uptake of ^{68}Ga-NODAGA-RGD into murine PDAC in *CKP* animals. Every bar represents PDAC of 1 animal. BW = body weight.
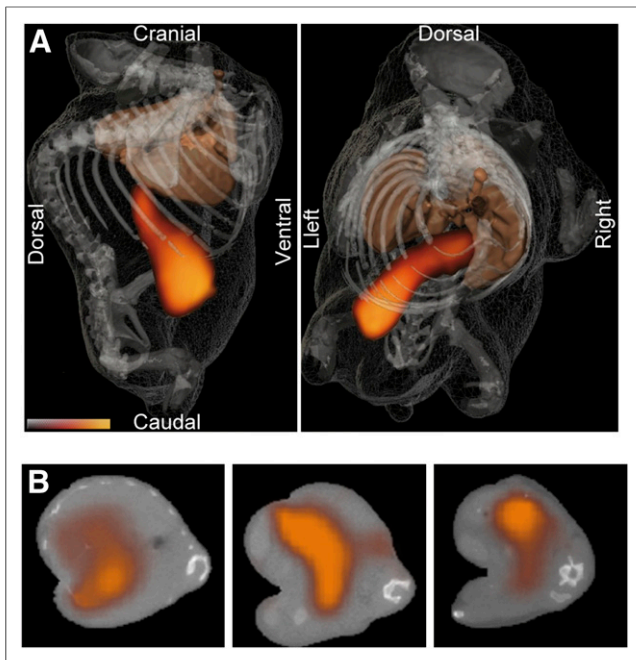
FIGURE 3. In vivo imaging using FMT-XCT. (A) Three-dimensional representations of reconstructed fluorescence signal along with anatomic data; segmented skeleton and lungs (brown isosurface) are shown from side and top views, respectively. Bottom left is gated color map with orange color for high signal values, as detected in PDAC. (B) Reconstructed fluorescence overlaid as pseudo-orange transparency on corresponding CT slices in 3 different positions in mouse body.

For validation of intraoperative and FMT-XCT imaging results, we used a recently developed ex vivo multispectral cryoslicing system (*24*). In animals with PDAC, fluorescence images of cryosections demonstrated strong and specific fluorescence signals in the tumor (Fig. 4C). Fluorescence accumulation at the tumor rims was not observed, and axial fluorescent images of the tumor correlated well with the axial T2w MR images, suggesting good probe penetration and binding in the tumor. Furthermore, cryoslicing confirmed the intraoperative observations of enhanced demarcation of tumor borders (Fig. 4C; Supplemental Fig. 1). The tumor was distinguishable from the surrounding organs. Some fluorescence was observable in various parts of the gut. However, tumor fluorescence was consistently stronger than that of the gut.

Microscopic analysis of cryoslides confirmed specific accumulation of IntegriSense in PDAC (Fig. 4D). Fluorescence signals for IntegriSense were observable around the $\beta3^+$ cells in PDAC, suggesting specific probe deposition in $\beta3^+$ areas of the tumor.

DISCUSSION

Recent breakthroughs in oncologic research have highlighted that traditional approaches to cancer as a whole organ must be remodeled and adapted to the fact that cancers are extremely complex and heterogeneous, necessitating deeper molecular characterization for personalized therapeutic approaches (*26*). Molecular imaging approaches that allow imaging and delineation of tumors and identification of clinically relevant subtypes are thus promising new imaging strategies. Our study suggests $\alpha_v\beta_3$ integrin to be one of the molecular targets suitable for such approaches as substantiated with the several imaging results presented in this work.

The clinical relevance of $\alpha_v\beta_3$ integrin is mirrored in the fact that patients whose cancer cells express $\alpha_v\beta_3$ have increased metastasis to lymph nodes and worse survival than those without $\alpha_v\beta_3$ expression (*14,15*). This was further confirmed in animal experiments, in which overexpression of $\alpha_v\beta_3$ led to enhanced primary tumor growth of orthotopic transplanted pancreatic cancer cells and enhanced metastatic potential, whereas $\alpha_v\beta_3$ knock-down diminished these actions (*14*).

For analysis of $\alpha_v\beta_3$ integrin expression in human PDAC, we performed immunohistochemistry for the integrin $\beta3$ subunit. $\beta3$ integrin dimerizes only with 2 different α integrins, αv and αIIb. αIIb integrin is specifically expressed on blood platelets (*27*), and it is thus generally accepted that $\beta3$ expression pattern in other tissues represents the expression of the $\alpha_v\beta_3$ dimer. Similar to previously published data on $\beta3$ expression found in 58% of human PDACs (*15*), we also found an increased expression of $\alpha_v\beta_3$ in a subpopulation of human PDAC (31%). In previously published studies and our study, the staining was found in cancer cells. The differences in the percentage of $\beta3^+$ PDAC can probably be attributed to limited total number of samples used in both studies (50 and 77). Heterogeneity in expression level and in localization of $\beta3$ among PDAC samples was observed as described previously (*14,15*). With the previously mentioned role of $\alpha_v\beta_3$ in metastatic potential of pancreatic cancer cells, this result suggests that the $\alpha_v\beta_3$ receptor might have an important biologic function and is potentially suitable for personalized targeted therapeutic approaches based on $\alpha_v\beta_3$ status.

As in humans, increased expression of $\alpha_v\beta_3$ was observed in murine PDAC. CKP animals used in this study recapitulate the human disease well, developing moderately differentiated, invasive PDAC with dense stroma (*28*). Most of the $\beta3$ expression in murine PDACs could be attributed to malignant (tumor) cells or reactive stroma. The different expression pattern of $\beta3$ and CD31, a marker of blood vessels, suggested that only a minor part of $\beta3^+$ cells actually belongs to the vascular compartment. Thus, although molecular imaging of $\alpha_v\beta_3$ is usually used for detection of tumor angiogenesis (*13*), targeting $\alpha_v\beta_3$ in murine PDAC would rather detect the tumor itself.

As a clinically relevant and applicable approach, we used PET imaging for $\alpha_v\beta_3$ detection in murine PDAC. Of many available $\alpha_v\beta_3$-targeting RGD tracers, a novel ^{68}Ga-labeled NODAGA-conjugated RGD peptide was chosen because of its easy accessibility, high stability, and previously reported good imaging properties (*17,29*). Furthermore, it has already been demonstrated that ^{68}Ga-labeled NODAGA-RGD accumulates to a small degree into the wild-type pancreas (*29*), making this agent suitable for specific detection of tumorous pancreatic tissue. PET imaging with ^{68}Ga-labeled NODAGA-RGD allowed good identification of murine PDAC. Imaging was further confirmed by accumulation of ^{68}Ga-labeled NODAGA-RGD in PDAC in the biodistribution study. Furthermore, efficient block of ^{68}Ga-NODAGA-RGD binding to $\alpha_v\beta_3$ by cilengitide confirmed the specificity of ^{68}Ga-NODAGA-RGD for $\alpha_v\beta_3$ integrin in PDAC. Accumulation ranged from 2% to 10% of injected dose in different experiments, and we assume that these small differences do not reflect heterogeneity in $\alpha_v\beta_3$ expression levels but can rather be attributed to varying size of the tumors and technical aspects.

In light of the recent success of fluorescence-based technologies for detection of $\alpha_v\beta_3$-positive ($\alpha_v\beta_3^+$) xenotransplanted cancers (*30,31*), we investigated whether better detection of PDAC is achievable with optical imaging, namely a novel noninvasive hybrid
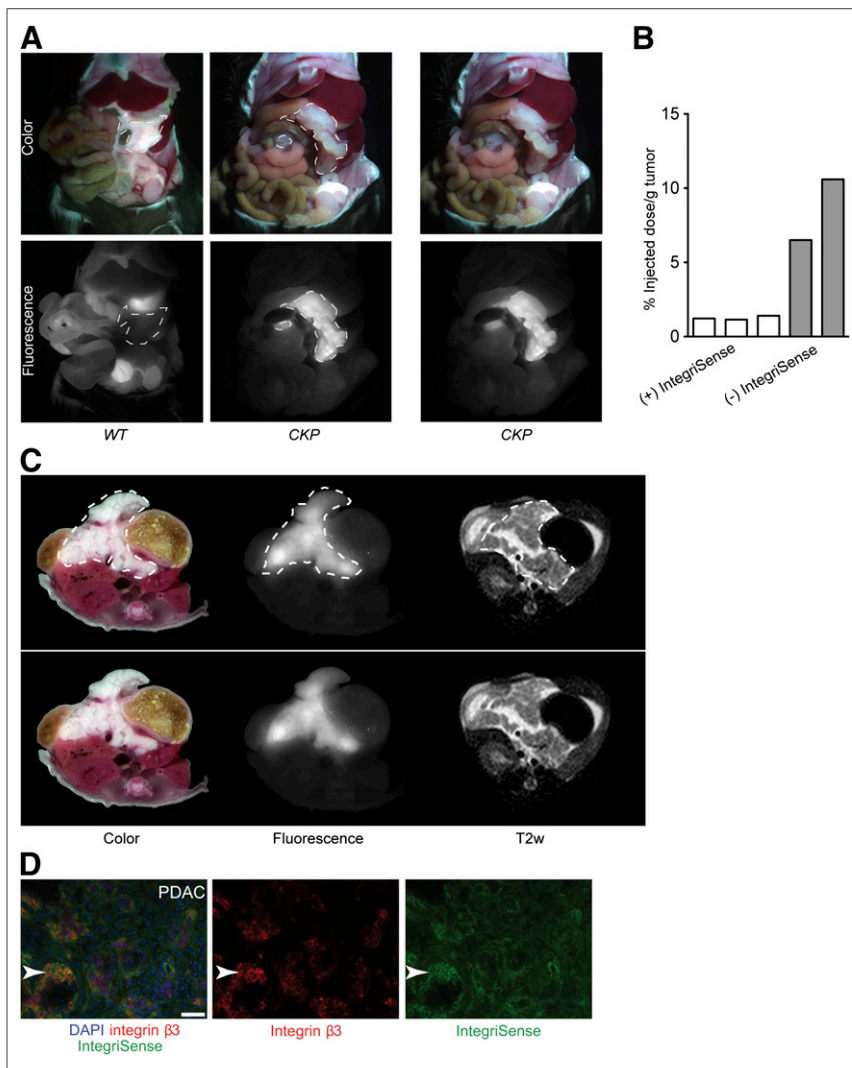
FIGURE 4. In vivo intraoperative and ex vivo cryoslicing optical imaging of IntegriSense in murine PDAC. (A) Representative planar epi-illumination whole-body color autopsy and original fluorescence images of wild-type and *CKP* animals. Tumor or pancreas area is lined with dotted white line (left), and tumor images are repeated without delineation (right). Strong equally distributed IntegriSense 680 fluorescence signals are detectable at tumor surface in *CKP* animals and no signals from wild-type pancreata. In wild-type animals, bladder visibly fluoresces due to probe clearance through the urinary system. (B) Injection of IntegriSense 24 h before injection of ^{68}Ga-NODAGA-RGD decreases uptake of ^{68}Ga-NODAGA-RGD into murine PDAC. Every bar represents 1 animal. (C) Representative whole-body axial cryoslicer images: color, fluorescence, and corresponding T2w images for *CKP* animal. Tumor is delineated with white dotted line. In *CKP* animals, axial T2w and fluorescence images correlated well, but delineation of tumor borders was better on fluorescence images. Images without delineation for readers' comfort (lower). (D) Microscopic analysis of IntegriSense distribution in PDAC. In *CKP* animals, IntegriSense accumulated in tumors. IntegriSense fluorescence (green) correlated well with β3 staining (red), demonstrating specific IntegriSense accumulation in β3[+] areas. Scale bar: 50 μm. WT= wild-type.

imaging method combining CT (XCT) with FMT (*21*) using IntegriSense 680 as a probe. Optical imaging with $\alpha_v\beta_3$-targeted probes was also successful in identification of PDAC. Although FMT is not yet widely adopted for clinical use, the future application of nonradiating, inexpensive, fluorescent probes is easy to envisage. The FMT-XCT offers superposition of anatomic and molecular information, the latter obtained from fluorescence agents, and has recently been reported as successful for the detection of murine lung tumors (*21*). By using XCT information in the FMT inversion, this hybrid approach also offers the most accurate FMT performance

to date (*21*). In our study, FMT performance was superior to PET, with specific signals detected from PDAC, suggesting that this method is a promising method of choice for future noninvasive identification of patients with $\alpha_v\beta_3^+$ cancers and thus identification of PDAC with higher metastatic potential.

The clear definition of surgical margins and complete operative removal of residual tissue are keys to PDAC treatment. Residual cancer tissues missed during surgery present a potential for cancer relapse. In the case of patients with resectable PDAC, translation of PET or FMT images into the operating room is a major challenge for the performing surgeon who needs on-site imaging assistance for surgery. Recently, van Dam et al. performed the first fluorescence-guided surgical approach in ovarian cancer patients and provided the first proof of principle for implementation of this technique in surgical practice (*7*). For this reason, we optimized an optical imaging approach suitable for potential intraoperative purposes with a fluorescent molecular probe targeting the $\alpha_v\beta_3$ integrin. Several $\alpha_v\beta_3$-targeting fluorescently labeled RGD molecules with different chemical and molecular properties have been developed and used for optical imaging in various xenograft cancer mouse models (*32–34*). IntegriSense 680 used in this study is commercially available and with good described specificity for $\alpha_v\beta_3$ integrin (*35*). Our competitive studies with ^{68}Ga-NODAGA-RGD also suggested specific binding of IntegriSense for integrin $\alpha_v\beta_3$.

IntegriSense has been previously used for fluorescence-guided surgery in xenograft cancer models (*30,31*). To our knowledge, it has not been evaluated in endogenous cancer mouse models. Intraoperative optical imaging of the abdomen showed specific IntegriSense signals at the tumor surface. Some unspecific fluorescence was observed on the surface of other organs, mostly gut, probably due to unspecific probe accumulation and food autofluorescence. Furthermore, intraoperative and FMT images were confirmed by ex vivo fluorescence imaging under cryosectioning that enables the detailed evaluation of probe biodistribution inside the tissue and comparison to other surrounding organs. Multispectral cryoslicing confirmed good probe penetration and specific intratumoral distribution and no unspecific probe accumulation at the tumor rims that could account for false-positive signals from tumor surface in intraoperative imaging. Thus, IntegriSense-guided intraoperative imaging may be of use for endoscopic evaluation and to navigate removal of PDAC aiming to minimize the amount of residual cancer tissue.

CONCLUSION

We showed that $\alpha_v\beta_3$ integrin is expressed in human and murine PDAC and can be detected by molecular imaging technologies in PDAC of GEMM. This strategy can further be exploited for identification of patients with $\alpha_v\beta_3^+$ PDAC, fluorescence-guided surgical removal of PDAC, and application of $\alpha_v\beta_3$-targeted therapies.

REFERENCES

1. Hidalgo M. Pancreatic cancer. *N Engl J Med.* 2010;362:1605–1617.
2. Tummala P, Junaidi O, Agarwal B. Imaging of pancreatic cancer: an overview. *J Gastrointest Oncol.* 2011;2:168–174.
3. Herrmann K, Erkan M, Dobritz M, et al. Comparison of 3′-deoxy-3′-[18F] fluorothymidine positron emission tomography (FLT PET) and FDG PET/CT for the detection and characterization of pancreatic tumours. *Eur J Nucl Med Mol Imaging.* 2012;39:846–851.
4. Nguyen NQ, Bartholomeusz DF. 18F-FDG-PET/CT in the assessment of pancreatic cancer: is the contrast or a better-designed trial needed? *J Gastroenterol Hepatol.* 2011;26:613–615.
5. Ntziachristos V. Going deeper than microscopy: the optical imaging frontier in biology. *Nat Methods.* 2010;7:603–614.
6. Keereweer S, Kerrebijn JD, van Driel PB, et al. Optical image-guided surgery: where do we stand? *Mol Imaging Biol.* 2011;13:199–207.
7. van Dam GM, Themelis G, Crane LM, et al. Intraoperative tumor-specific fluorescence imaging in ovarian cancer by folate receptor-alpha targeting: first in-human results. *Nat Med.* 2011;17:1315–1319.
8. Keliher EJ, Reiner T, Earley S, et al. Targeting cathepsin E in pancreatic cancer by a small molecule allows in vivo detection. *Neoplasia.* 2013;15:684–693.
9. Eser S, Messer M, Eser P, et al. In vivo diagnosis of murine pancreatic intraepithelial neoplasia and early-stage pancreatic cancer by molecular imaging. *Proc Natl Acad Sci USA.* 2011;108:9945–9950.
10. Cruz-Monserrate Z, Abd-Elgaliel WR, Grote T, et al. Detection of pancreatic cancer tumours and precursor lesions by cathepsin E activity in mouse models. *Gut.* 2012;61:1315–1322.
11. Neesse A, Hahnenkamp A, Griesmann H, et al. Claudin-4-targeted optical imaging detects pancreatic cancer and its precursor lesions. *Gut.* 2013;62:1034–1043.
12. Desgrosellier JS, Cheresh DA. Integrins in cancer: biological implications and therapeutic opportunities. *Nat Rev Cancer.* 2010;10:9–22.
13. Beer AJ, Schwaiger M. Imaging of integrin alphavbeta3 expression. *Cancer Metastasis Rev.* 2008;27:631–644.
14. Desgrosellier JS, Barnes LA, Shields DJ, et al. An integrin $\alpha_v\beta_3$-c-Src oncogenic unit promotes anchorage-independence and tumor progression. *Nat Med.* 2009;15:1163–1169.
15. Hosotani R, Kawaguchi M, Masui T, et al. Expression of integrin alphaVbeta3 in pancreatic carcinoma: relation to MMP-2 activation and lymph node metastasis. *Pancreas.* 2002;25:e30–e35.
16. Beer AJ, Haubner R, Sarbia M, et al. Positron emission tomography using [18F] Galacto-RGD identifies the level of integrin $\alpha_v\beta_3$ expression in man. *Clin Cancer Res.* 2006;12:3942–3949.
17. Knetsch PA, Petrik M, Griessinger CM, et al. [68Ga]NODAGA-RGD for imaging $\alpha_v\beta_3$ integrin expression. *Eur J Nucl Med Mol Imaging.* 2011;38:1303–1312.
18. Nakhai H, Sel S, Favor J, et al. Ptf1a is essential for the differentiation of GABAergic and glycinergic amacrine cells and horizontal cells in the mouse retina. *Development.* 2007;134:1151–1160.
19. Hingorani SR, Petricoin EF, Maitra A, et al. Preinvasive and invasive ductal pancreatic cancer and its early detection in the mouse. *Cancer Cell.* 2003;4:437–450.
20. Marino S, Vooijs M, van Der Gulden H, Jonkers J, Berns A. Induction of medulloblastomas in p53-null mutant mice by somatic inactivation of Rb in the external granular layer cells of the cerebellum. *Genes Dev.* 2000;14:994–1004.
21. Ale A, Ermolayev V, Herzog E, Cohrs C, de Angelis MH, Ntziachristos V. FMT-XCT: in vivo animal studies with hybrid fluorescence molecular tomography-X-ray computed tomography. *Nat Methods.* 2012;9:615–620.
22. Schulz RB, Ale A, Sarantopoulos A, et al. Hybrid system for simultaneous fluorescence and x-ray computed tomography. *IEEE Trans Med Imaging.* 2010;29:465–473.
23. Themelis G, Yoo JS, Soh KS, Schulz R, Ntziachristos V. Real-time intraoperative fluorescence imaging system using light-absorption correction. *J Biomed Opt.* 2009;14:064012.
24. Sarantopoulos A, Themelis G, Ntziachristos V. Imaging the bio-distribution of fluorescent probes using multispectral epi-illumination cryoslicing imaging. *Mol Imaging Biol.* 2011;13:874–885.
25. Burke PA, DeNardo SJ, Miers LA, Lamborn KR, Matzku S, DeNardo GL. Cilengitide targeting of $\alpha_v\beta_3$ integrin receptor synergizes with radioimmunotherapy to increase efficacy and apoptosis in breast cancer xenografts. *Cancer Res.* 2002;62:4263–4272.
26. Gerlinger M, Rowan AJ, Horswell S, et al. Intratumor heterogeneity and branched evolution revealed by multiregion sequencing. *N Engl J Med.* 2012;366:883–892.
27. Ma YQ, Qin J, Plow EF. Platelet integrin alpha(IIb)beta(3): activation mechanisms. *J Thromb Haemost.* 2007;5:1345–1352.
28. Bardeesy N, Aguirre AJ, Chu GC, et al. Both p16(Ink4a) and the p19(Arf)-p53 pathway constrain progression of pancreatic adenocarcinoma in the mouse. *Proc Natl Acad Sci USA.* 2006;103:5947–5952.
29. Pohle K, Notni J, Bussemer J, Kessler H, Schwaiger M, Beer AJ. 68Ga-NODAGA-RGD is a suitable substitute for (18)F-Galacto-RGD and can be produced with high specific activity in a cGMP/GRP compliant automated process. *Nucl Med Biol.* 2012;39:777–784.
30. Themelis G, Harlaar NJ, Kelder W, et al. Enhancing surgical vision by using real-time imaging of $\alpha_v\beta$. *Ann Surg Oncol.* 2011;18:3506–3513.
31. Harlaar NJ, Kelder W, Sarantopoulos A, et al. Real-time near infrared fluorescence (NIRF) intra-operative imaging in ovarian cancer using an $\alpha_v\beta_3$-integrin targeted agent. *Gynecol Oncol.* 2013;128:590–595.
32. Wu Y, Cai W, Chen X. Near-infrared fluorescence imaging of tumor integrin alpha v beta 3 expression with Cy7-labeled RGD multimers. *Mol Imaging Biol.* 2006;8:226–236.
33. Chen X, Conti PS, Moats RA. In vivo near-infrared fluorescence imaging of integrin $\alpha_v\beta_3$ in brain tumor xenografts. *Cancer Res.* 2004;64:8009–8014.
34. Wang W, Ke S, Wu Q, et al. Near-infrared optical imaging of integrin $\alpha_v\beta_3$ in human tumor xenografts. *Mol Imaging.* 2004;3:343–351.
35. Kossodo S, Pickarski M, Lin SA, et al. Dual in vivo quantification of integrin-targeted and protease-activated agents in cancer using fluorescence molecular tomography (FMT). *Mol Imaging Biol.* 2010;12:488–499.